Nonlinear Analysis of Snapping Hyperelastic Prestressed Arches

Filipe Fonseca[1], Paulo B. Gonçalves[1]

[1]*Dept. of Civil and Environmental Engineering, Pontifical Catholic University of Rio de Janeiro*
Rua Marquês de São Vicente, 225, Gávea, 22453-900, RJ, Brazil
filipemfonseca19@gmail.com, paulo@puc-rio.br

Abstract. Over the past decades, a variety of applications of multistable structures has appeared in different branches of engineering. Among the structures exhibiting multistability, metamaterials, formed by a sequence of structures able to undergo large displacements and deformations without presenting damage, thus being able to assume different equilibrium positions, are investigated in the current literature. Many of these structures display a nonlinear behavior with limit point instability, allowing the structure to jump between various stable equilibrium positions and thus present a reversible hysteretic behavior. Among the materials used in this type of structure are hyperelastic materials. In this work, the behavior of hyperelastic arches obtained from buckled columns in a post-buckling configuration, under transversal loads, is studied; a bistable structural unit typical of metamaterials. To understand the nonlinear behavior of these structures, a finite element model is used by means of the Abaqus software that allows specifying several constitutive laws commonly used for hyperelastic materials. To obtain non-linear equilibrium paths, the Riks method is applied. A parametric analysis of the nonlinear behavior of the arch shows the influence of the geometry of the arch (height-to-span ratio and thickness), self-weight and load imperfections on the nonlinear equilibrium paths, load capacity (critical load) and stored energy of the structure.

Keywords: Incompressible material, hyperelastic prestressed arch, instability, snap-through, finite element analysis.

1 Introduction

The study of the multistability of arch-shaped structures has received new interests in recent decades due to their new applications in different fields of engineering, such as mechanical metamaterials [1-3], vibration control [4,5] and morphing applications through bistable mechanisms [6-8], among others. A review of the state of the art in exploring multi-stability in structures formed by metamaterials and their structural transitions is presented by Kochmann and Bertoldi [9]. In most of these applications, the structural element is subjected to large deformations, and it is often important to consider in its formulation or modeling, materials capable of undergoing large elastic deformations. Under these conditions, the use of hyperelastic materials finds an important field of application. The hyperelasticity of the material increases the deformation capacity of structure, leading to new deformations at the section level [10] and, consequently, new equilibrium trajectories accompanied by limit point instability with multiple self-equilibrated load-free configurations and a complex potential energy landscape [11].

In this work, the behavior of hyperelastic arches obtained from columns in a post-buckling configuration, under transversal loads, is studied; a bistable structural system typical of metamaterials. To understand the nonlinear behavior of these structures, a finite element model is used by means of the Abaqus Unified FEA [12] using an incompressible Mooney-Rivlin model obtained from experimental uniaxial tests of a rubber-like material. To obtain non-linear equilibrium paths, the Riks method [13] is applied. A parametric analysis of the nonlinear behavior of the arches shows the influence of boundary conditions, different cross-sections, self-weight and load imperfections on the nonlinear equilibrium paths and stability of the structure, highlighting some key features of this class of structures.

2 Problem and analysis

Consider a hyperelastic column of rectangular cross-section with base B and height H, undeformed length, L, and clamped or pinned at both ends. After being subjected to buckling by an imposed horizontal displacement, δ, it takes the form of a pre-stressed arch, as illustrated in Figure 1. Then it is subjected to an incremental vertical load (P) applied at the top of the arch. The pinned arch has an initial rotation θ at the support. The resulting arch has a height h and a span (L- δ), as shown in Table 1, considering L=450mm.

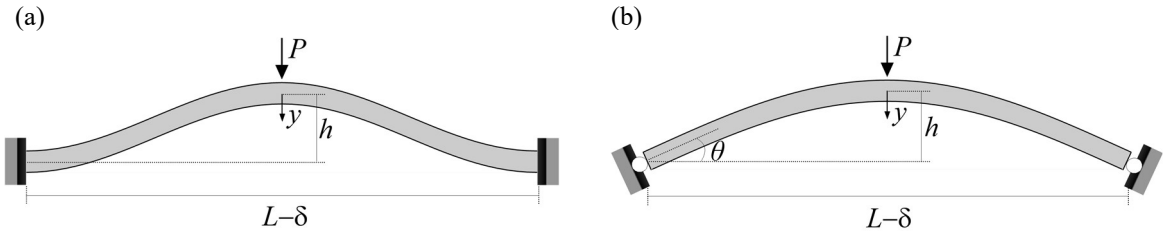

Figure 1. Hyperelastic prestressed arches with (a) clamped and (b) pinned supports.

Table 1. Arch geometry (L=450mm)

Support	δ (mm)	h (mm)	θ (degrees)
clamped	10	34.14	0
	30	67.89	0
	50	88.70	0
pinned	10	40.09	16.40
	30	70.92	29.42
	50	90.90	38.38

2.1 Uniaxial tests of a rubber-like material

The columns are made of an incompressible elastomer with physical properties obtained experimentally. The elastomer has density of 1480 kg/m³. Hyperelastic incompressible materials are highly nonlinear, with different behaviors under tension and compression, and their constants depends on the proportion of the constituent elements and fabrication process. Its mechanical properties are determined through a series of uniaxial tensile and compression tests, as illustrated in Fig. 2(a), conducted at the Civil Engineering Department material and structures laboratory (LEM) of PUC-Rio.

The experimental results of the nominal stress (σ_{eng}) as a function of the principal axial stretch (λ_1) are shown in Figure 2(b). The material constitutive equation is obtained by a fitting process using the Abaqus Unified FEA software considering a deformation domain whose limit is the maximum deformation levels that the structures are submitted to in the numerical analysis. The best fit was obtained for the Mooney-Rivlin hyperelastic model (MR). The Mooney-Rivlin strain energy density function for an incompressible material is written in terms of the first and second strain invariants, I_1 and I_2, which can be expressed as a function of the principal stretch ratios of the structural element, λ_i, and the material constants C_1 and C_2 [10,14]:

$$W = \mathrm{C}_1(I_1 - 3) + \mathrm{C}_2(I_2 - 3). \quad (1)$$

The Mooney-Rivlin constitutive model is widely used for rubber within a moderate strain range (up to 200%) as those observed during the numerical analysis [14]. The experimental parameters here obtained are equal to C_1=0.3734 MPa and C_2=0.1726 MPa.

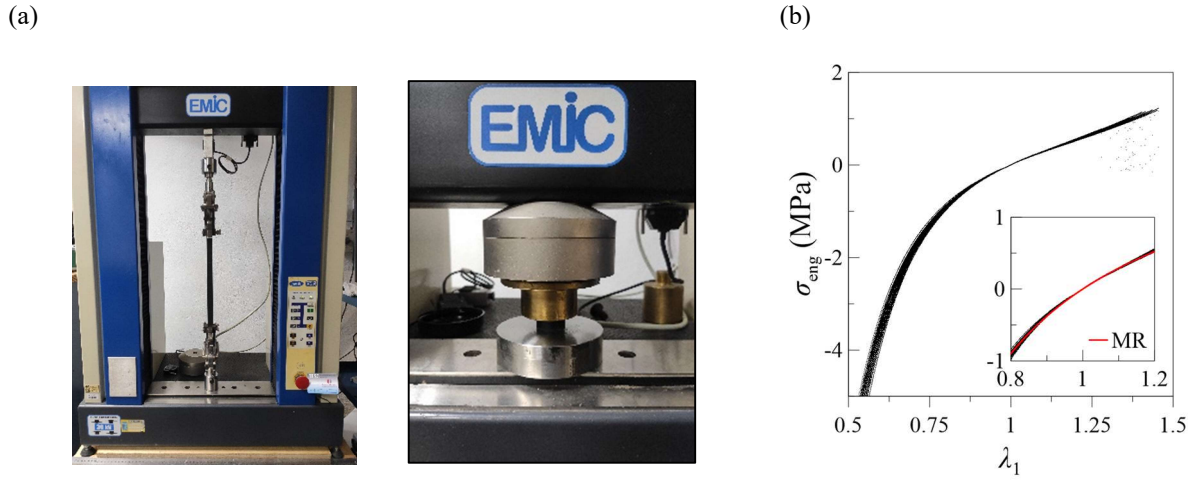

Figure 2. (a) Tensile and compression tests and (b) model fitting

2.2 Finite element model

The column was modeled using the Abaqus Unified FEA [12]. A 3-node quadratic Timoshenko beam element (*B22*) is adopted to model the beam. The problem is modeled in two steps. In the first one, assuming a small initial imperfection in the shape of the first buckled mode of the clamped and pinned beam, the delta displacement (δ) is applied to the beam tip (Figure 1) and, in the following step, the nonlinear response and stability analysis of the buckled beam is performed through the Riks method [13].

2.3 Results and discussion

The arch non-linear behavior when subjected to transversal loads depends on the shallowness parameter defined as the height-to-span ratio, leading to different instability phenomena along their primary equilibrium path, namely: symmetric bifurcation or limit point instability. These instability phenomena divide these structures in two classes: non-shallow (deep) arches and shallow arches [15], respectively. These structures are commonly adopted in the design of metamaterials and bistable applications where the snap-through phenomena allow the structure to jump dynamically from one to another equilibrium position storing or releasing energy. Consider a prestressed arch with clamped supports, L=450 mm, B=43.72 mm and H=21.79 mm, subject to three initial displacement, respectively δ=10, 30, 50 mm. Their nonlinear equilibrium paths are shown in Fig. 3a.

As shown in Fig.3a, as the load increases, the arch effective stiffness decreases due to the softening geometric nonlinearity of the structure. Upon reaching the critical load, the effective stiffness becomes zero and then, under any load increment, the compressed arch jumps to an inverted equilibrium position where it is subjected to traction. For δ=10 mm (very shallow arch) there are 3 self-equilibrated load-free configurations, as delta increases the structure presents an increasing number of self-equilibrated load-free configurations due to an increasing number of loops. Two positions are always stable (minima), and the others are unstable (saddles or maxima). These points are clarified in Fig. 3b where the variation of the load (in blue) and the strain energy (in black) with the central deflection are shown for δ=50 mm. The five symmetrical self-equilibrated load-free configurations are shown inset in black. The critical configuration is also illustrated in green. Unstable positions and those close to them are configurations of high energy under null or low force, making these positions highly indicated for storing energy.

The equilibrium paths of the arch with pinned supports are more complex with several loops and self-equilibrated load-free equilibrium positions. Figure 4 shows the equilibrium paths and the self-equilibrated positions for the pinned prestressed arch (B=43.72 mm, H=21.79 mm) for different axial displacements δ.

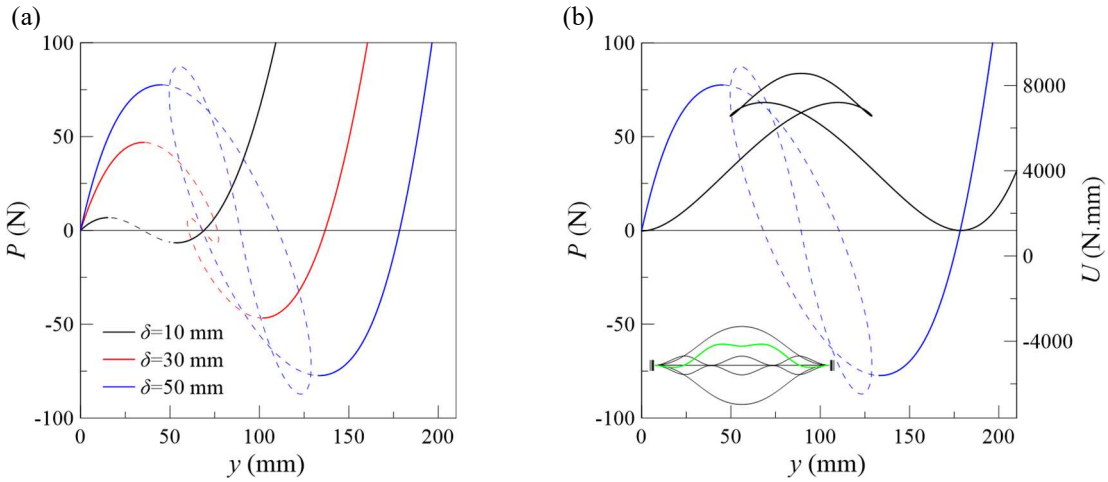

Figure 3. Clamped prestressed arch (L=450 mm, B=43.72 mm, H=21.79 mm): (a) equilibrium paths (δ=10, 30, 50 mm); (b) load (blue) and strain energy (black) versus vertical displacement (δ=50 mm).

For the smallest δ value, δ=10 mm, the structure has five self-equilibrated load-free configurations (in black in Fig. 4b) and upon reaching the critical load (green curve in Fig. 4b) jumps to its stable post-critical position. As δ increases the complexity of the equilibrium path increases and the reaches up to eleven self-equilibrated load-free configurations for δ=50 mm (Fig. 4(c)). Figs. 4(c,d) show the characteristic shape of the critical configuration in green. Close to the supports, the structure moves upwards instead of downwards. However non-shallow arches lose stability due to an unstable symmetric bifurcation before the limit point is attained.

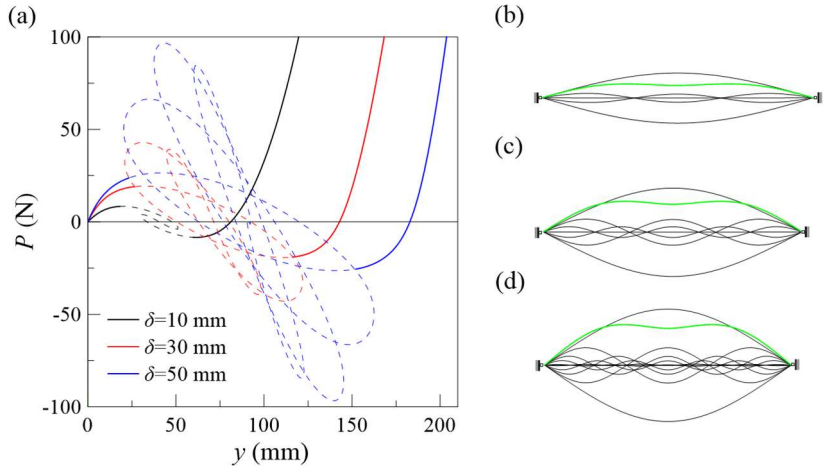

Figure 4. (a) Equilibrium paths (δ=10, 30, 50 mm); (b), (c), (d) self-equilibrated load-free and critical configurations of pinned prestressed arch (L=450 mm, B=43.72 mm, H=21.79 mm) for δ=10, 30, 50 mm, respectively.

Rubber-like materials have lower values for Young's modulus to density ratio than other materials and it is important to include their self-weight in the structural analysis. Figure 5 shows the equilibrium paths for the clamped prestressed arch with δ=50 mm. The inclusion of the self-weight reduces the load capacity of the structure by 35%, as shown by the curve in black when compared to the ideal case without considering self-weight in gray. The loss of stability is by limit point due to the inherent symmetry of the system. When self-weight and load imperfection (considering an eccentricity at the load application point of 5 mm to the left of the symmetry point) the load capacity is reduced by 66% when compared to the ideal case without considering self-weight. This eccentricity causes the complete loss of structural symmetry, as illustrated in the equilibrium and critical configurations shown respectively in black and green inset in Fig. 5. Another interesting feature of rubber-like

materials is their high flexibility, which allows the elastomer arches to be subjected to higher levels of elastic deformation than conventional structures without any damage, enabling the structure to jump to an inverted position in the elastic regime, which cannot usually occur for structural material such as the steel arches tested by Neville et al [16, 17], unless they are extremely slender and shallow. Figure 6 shows the influence of boundary conditions, section height (different values of H/B), self-weight and load imperfections on the critical buckling load. It is observed that the H/B ratio, that is, the slenderness of the cross-section, has a significant influence on the load carrying capacity, which increases as H/B increases. In each case, the consideration of self-weight and self-weight plus load imperfections causes, as illustrated in Fig. 5, a decrease in the load carrying capacity. This shows that self-weight must be always included in the analysis of these structures and that they exhibit a significant imperfection sensitivity. Thus, the effect of imperfections must be considered with care in their analysis and design.

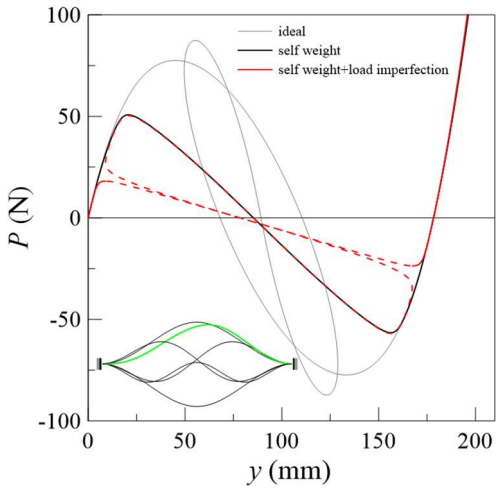

Figure 5. Effect of load imperfection and self-weight on the equilibrium paths (L=450 mm, B=43.72 mm, H=21.79 mm, δ=50 mm).

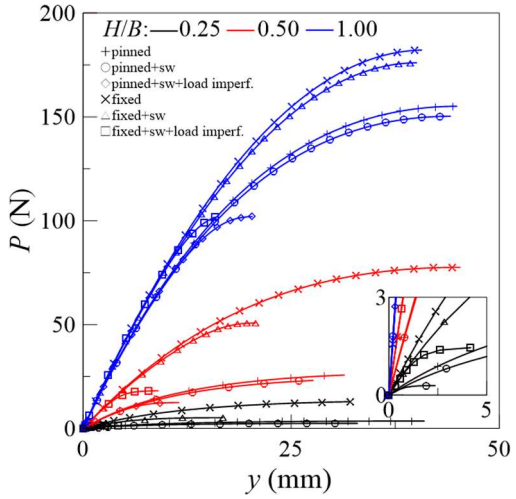

Figure 6. Effect of load imperfection and self-weight on critical load (L=450 mm, B=43.72 mm, H(variable)).

3 Conclusions

This article examines the bistable behavior of a hyperelastic arches. Fabrication and testing of a rubber-like material were conducted to identify the material physical properties and the best constitutive model. A parametric analysis of arches under transversal load was performed by varying its section height, height-to-span ratio, and boundary conditions using the Abaqus Unified FEA, highlighting the key features to understand the mechanical behavior of the arches in multistable applications. The clamped and pinned arches analyzed here exhibit a mechanical behavior that defines the upper and lower bounds of a typical unit. The parametric analysis carried out here also show that self-weight and load imperfections have a significant influence on the bistable behavior and load capacity of rubber-like structures. Thus, the presents results allow to understand the real non-linear behavior of the hyperelastic structures used in bistable applications. Future work will include the experimental analysis of the clamped and pinned hyperelastic arches.

Acknowledgements. The authors acknowledge the financial support of the Brazilian research agencies CAPES [finance code 001 and 88881.310620/2018-01], CNPq [grant number 301355/2018-5], FAPERJ-CNE [grant number E-26/202.711/2018] and FAPERJ Nota 10 [grant number E-26/200.619/2021].

Authorship statement. The authors hereby confirm that they are the sole liable persons responsible for the authorship of this work, and that all material that has been herein included as part of the present paper is either the property (and authorship) of the authors, or has the permission of the owners to be included here.

References

[1] Rafsanjani, A., Akbarzadeh, A., and Pasini, D. "Snapping mechanical metamaterials under tension". *Advanced Materials*, v. 27, n. 39, p. 5931-5935, 2015.
[2] Shan, S. et al. "Multistable architected materials for trapping elastic strain energy". *Advanced Materials*, v. 27, n. 29, p. 4296-4301, 2015.
[3] Yang, H., Ma, L. "Multi-stable mechanical metamaterials by elastic buckling instability". Journal of materials science, v. 54, n. 4, p. 3509-3526, 2019.
[4] Virgin, L. N., Davis, R. B. "Vibration isolation using buckled struts". *Journal of Sound Vibration*, v. 260, n. 5, p. 965-973, 2003.
[5] Huang, X. et al. "Shock isolation performance of a nonlinear isolator using Euler buckled beam as negative stiffness corrector: Theoretical and experimental study". Journal of Sound and Vibration, v. 345, p. 178-196, 2015.
[6] Diaconu, Cezar G.; Weaver, P. M., Mattioni, F. "Concepts for morphing airfoil sections using bi-stable laminated composite structures". *Thin-Walled Structures*, v. 46, n. 6, p. 689-701, 2008.
[7] Zirbel, S. A., Tolman, K. A., Trease, B. P., and Howell, L. L. "Bistable mechanisms for space applications". *PloS one*, v. 11, n. 12, p. e0168218, 2016.
[8] Cui, Y., Santer, M. "Highly multistable composite surfaces". *Composite Structures*, 124, 44-54, 2015.
[9] Kochmann, D. M.; Bertoldi, K. Exploiting microstructural instabilities in solids and structures: from metamaterials to structural transitions. *Applied Mechanics Reviews*, v. 69, n. 5, 2017.
[10] Fonseca F., Gonçalves P. B. Nonlinear analysis of a hyperelastic beam in pure bending. In: Proceedings of the XLI Ibero-Latin-American Congress on Computational Methods in Engineering, p. 1-7.
[11] Fonseca, F. Nonlinear behaviour, bifurcations, and instability of a hyperelastic truss. Dissertation, PUC-Rio, 2018.
[12] Systemes, D. Abaqus Unified FEA Software. 2017.
[13] Riks, E. "An incremental approach to the solution of snapping and buckling problems". *International journal of solids and structures*, v. 15, n. 7, p. 529-551, 1979.
[14] Marckmann, G. and Verron, E. "Comparison of hyperelastic models for rubber-like materials". *Rubber chemistry and technology*, vol. 79, n. 5, pp. 835-858, 2006.
[15] Bazant, Z. P., Cedolin, L. Stability of structures: elastic, inelastic, fracture and damage theories. World Scientific, 2010.
[16] Neville, R. M. et al. "Shape control for experimental continuation". *Physical review letters*, v. 120, n. 25, p. 254101, 2018.
[17] Neville, R. M. et al. "Beyond the fold: experimentally traversing limit points in nonlinear structures". *Proceedings of the Royal Society A*, v. 476, n. 2233, p. 20190576, 2020.